

2016

Refrigerant Distribution Characteristics in Vertical Header of Flat-Tube Heat Exchanger

Kazuhiro Endoh

Hitachi, Ltd., Japan, kazuhiro.endo.un@hitachi.com

Follow this and additional works at: <http://docs.lib.purdue.edu/iracc>

Endoh, Kazuhiro, "Refrigerant Distribution Characteristics in Vertical Header of Flat-Tube Heat Exchanger" (2016). *International Refrigeration and Air Conditioning Conference*. Paper 1695.
<http://docs.lib.purdue.edu/iracc/1695>

This document has been made available through Purdue e-Pubs, a service of the Purdue University Libraries. Please contact epubs@purdue.edu for additional information.

Complete proceedings may be acquired in print and on CD-ROM directly from the Ray W. Herrick Laboratories at <https://engineering.purdue.edu/Herrick/Events/orderlit.html>

Refrigerant Distribution Characteristics in Vertical Header of Flat-Tube Heat Exchanger

Kazuhiro ENDOH

Hitachi, Ltd., Research & Development Group
Hitachinaka, Ibaraki, Japan
E-mail: kazuhiro.endo.un@hitachi.com

ABSTRACT

A heat exchanger that arranges flat tubes horizontally has a vertical header that distributes the refrigerant to each tube. When the heat exchanger works as an evaporator, differences in flow conditions at each branch, such as the ratio and distribution of vapor and liquid, due to the differences in densities and momentums of vapor and liquid in the two-phase flow make equal distribution difficult. This paper describes the distribution characteristics of a four-branch header that has a rectangular cross-section without the internal protrusion of flat tubes in the case of the inflow of the refrigerant R32 from the bottom of the header by using an equipment that can estimate the distribution ratio of the liquid and vapor phase to each branch. This paper also discusses the distribution characteristics on the basis of the flow visualization in the header. The flow visualization shows that a liquid level that contains vapor phase exists in the header and affects the distribution greatly.

1. INTRODUCTION

To increase energy saving of air-conditioners, air-side pressure loss is being decreased and heat transfer coefficient is being increased due to the decrease in the dead-water region behind heat transfer tubes of the heat exchanger by reducing diameters of tubes or flattening them. This reduces the inner volume of the heat exchanger and results in the decrease in the amount of refrigerant used. On the other hand, the number of passes of the heat exchanger needs to be increased to suppress the increase in refrigerant-side pressure loss due to the decrease in the cross-sectional area of flow channel. At this time, the important issue is to distribute the refrigerant to each pass equally.

A multiport flat tube has a number of holes whose inner diameter is less than about 1mm. A heat exchanger that arranges these tubes horizontally has a vertical header that distributes the refrigerant to each tube. When the heat exchanger works as an evaporator, differences in flow conditions at each branch, such as the ratio and distribution of vapor and liquid, due to the differences in densities and momentums of vapor and liquid in the two-phase flow make equal distribution difficult.

The distribution of two-phase fluid in the vertical header of the flat-tube heat exchanger has been quantitatively evaluated and visualized. Lee (2009) studied the distribution characteristics of the air-water two-phase fluid entering the bottom of the header. However, since the physical properties of air-water two-phase fluid are very different from those of refrigerants, the findings cannot be applied to the header for refrigerants. Byun and Kim (2011) tested and visualized the refrigerant distribution in the vertical header made for simulating an actual evaporator. Zou and Hrnjak (2013, 2015) studied the distribution characteristics of the header with the internal protrusion of 10 flat tubes, where the refrigerant flows from the lower five flat tubes to the upper five flat tubes. However, Byun and Kim's and Zou and Hrnjak's flow channel geometries are too complicated for understanding the basic characteristics of the distribution of a vertical header. Furthermore, Zou and Hrnjak showed only the liquid phase distribution ratio and no vapor phase distribution ratio, and this is insufficient to understand details of distribution characteristics.

To understand the basic characteristics of the refrigerant distribution of a vertical header for a flat-tube heat exchanger, this paper describes the distribution characteristics of a four-branch header that has a rectangular cross-section without the internal protrusion of flat tubes in the case of the inflow of the refrigerant R32 from the bottom

of the header by using an equipment that can estimate the distribution ratio of the liquid and vapor phase to each branch. This paper also discusses the distribution characteristics on the basis of the flow visualization in the header.

2. EXPERIMENTAL SETUP AND TEST PROCEDURE

2.1 Configuration of Header

Figure 1 shows the configuration of a header used for the experiment, and Table 1 shows its specifications. Dimensions in Table 1 are normalized with the hydraulic diameter of the header. The header is made of stainless steel parts and glass for inside visualization, which are bolted for a change of structure. The inner cross-sectional shape of the header is a rectangle with an aspect ratio of 0.43. The vapor-liquid two-phase refrigerant flows from the bottom of the header to branch holes on the side of the header, which mimic a multiport of a flat tube and have a flat cross-sectional shape with an aspect of 0.11 with a dimensionless hydraulic diameter of 0.26. Although the header has eight branch holes, four of them are used by appressing a thin plate that opens every other holes or consecutive holes to the side of the header. The dimensionless branch pitch in the case for every other hole, which is 2.76, is defined as a standard one and the pitch for consecutive holes as a half one.

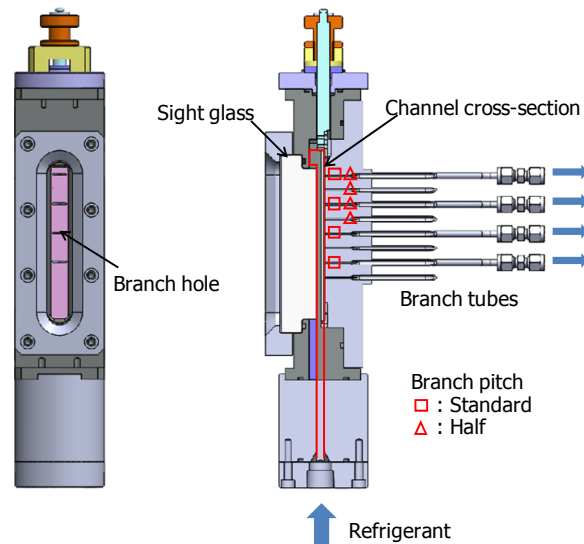


Figure 1: Configuration of header

Table 1: Specifications of header

| | | |
|-------------|----------------------------------|------------|
| Header | Inner cross-sectional shape | Rectangle |
| | Aspect ratio | 0.43 |
| | Dimensionless hydraulic diameter | 1 |
| | Number of branch | 4 |
| | Dimensionless branch pitch | 1.38, 2.76 |
| Branch hole | Cross-sectional shape | Flat |
| | Aspect ratio | 0.11 |
| | Dimensionless hydraulic diameter | 0.26 |

2.2 Experimental Setup and Test Procedure

Figure 2 shows the system diagram of the experimental setup for evaluating the refrigerant distribution of a four-branch header. The experimental setup consists of a compressor, an oil separator, a water-cooled condenser, a preheater, an expansion valve, a test header, and an evaporator that has four passes of heater-heated tubes and four straight tubes for measuring differential pressures. The powers of heaters for each pass of the evaporator are controlled in such a way that the temperatures of superheated vapor at the outlet of each pass are set at a predetermined value. Differential pressures of superheated vapors in straight tubes at the outlet of each pass are measured for estimating refrigerant flow rates.

A header inlet enthalpy i_{hi} needed for obtaining a header inlet quality x_{hi} is calculated as follows, using the condenser inlet enthalpy i_{ci} as a standard and representing the water heat exchange amount of the condenser as Q_w , the electric power of the preheater as W_{ph} , and the refrigerant flow rate as G_r .

$$i_{hi} = i_{ci} - (Q_w - W_{ph}) / G_r \quad (1)$$

The water-side heat exchange amount of the condenser Q_w is calculated as follows, using the heat capacity C_{pw} , the density ρ_w , the volume flow rate L_w , the outlet temperature T_{wo} , and the inlet temperature T_{wi} for water.

$$Q_w = C_{pw} \rho_w L_w (T_{wo} - T_{wi}) \quad (2)$$

The refrigerant flow rate in the No. i pass (branch) $G_{r,i}$ is estimated from a Blasius equation for friction factor as follows, using the differential pressure in a straight tube ΔP_i , the density ρ_i , and the viscosity μ_i .

$$G_{r,i} = \frac{k_i (\Delta P_i \rho_i \mu_i^{-0.25})^{1/1.75}}{\sum_{j=1}^4 k_j (\Delta P_j \rho_j \mu_j^{-0.25})^{1/1.75}} G_r \quad (3)$$

The correction factor k_i is for compensating for production variation of straight tubes. Since a total of refrigerant flow rates estimated from the differential pressures in the straight tubes of each pass are different from the refrigerant flow rate with the mass flowmeter G_r , the refrigerant flow rate in the No. i pass $G_{r,i}$ is corrected by multiplying the ratio.

An enthalpy of No. i branch of the header outlet (branch inlet) $i_{ho,i}$ needed for obtaining a quality of No. i branch inlet $x_{ho,i}$ is calculated as follows, using the outlet enthalpy of pass No. i evaporator (heater-heated tube) $i_{eo,i}$ and the electric power of No. i pass heater $W_{e,i}$.

$$i_{ho,i} = i_{eo,i} - \frac{W_{e,i}}{G_{r,i}} \frac{Q_e}{W_e} \quad (4)$$

Since the electric power of heater differs from the refrigerant-side heat exchange amount due to the effect of heat exchange with the surroundings, the electric power of No. i pass heater $W_{e,i}$ is corrected by the ratio of the refrigerant-side heat exchange amount Q_e to the total electric power of heaters W_e . Q_e and W_e are represented as follows.

$$Q_e = G_r (i_{eo} - i_{hi}) \quad (5)$$

$$W_e = \sum_{i=1}^4 W_{e,i} \quad (6)$$

The liquid phase flow rate of No. i branch of the header outlet $G_{r,l,i}$ and the vapor phase flow rate of that $G_{r,v,i}$ are represented as follows.

$$G_{r,l,i} = (1 - x_{ho,i}) G_{r,i} \quad (7)$$

$$G_{r,v,i} = x_{ho,i} G_{r,i} \quad (8)$$

Since the liquid phase refrigerant that has evaporative latent heat contributes to the cooling at the evaporator, the distribution ratio of liquid phase is important. The dimensionless standard deviation related to liquid phase flow rate

σ is used as an index for the distribution performance as follows, letting $\overline{G_{r_l}}$ be the arithmetic mean value of liquid phase flow rate.

$$\sigma = \frac{1}{\overline{G_{r_l}}} \sqrt{\frac{1}{4} \sum_{i=1}^4 (G_{r_l,i} - \overline{G_{r_l}})^2} \quad (9)$$

$$\overline{G_{r_l}} = \frac{1}{4} \sum_{i=1}^4 G_{r_l,i} \quad (10)$$

Table 2 shows test conditions at the header inlet. The refrigerant R32 was used and the saturated temperature was 15°C. The mass fluxes were set to 25, 50, and 75 kg/(m²s) for evaluating the effect of mass flux. The qualities were also set to 0.2, 0.4, and 0.6 for evaluating the effect of quality. To reduce the difference between the electric power of the heater and the refrigerant-side heat exchange amount at the evaporator, the experimental setup was installed in the temperature-controlled room at about 15°C, which is close to the refrigerant temperature at the header inlet. The difference between the total electric power of heaters W_e and the refrigerant-side heat exchange amount Q_e was within 3% at the mass flux of 50 kg/(m²s). The test conditions were set by adjusting the compressor speed, the water flow rate at the condenser, the opening of the expansion valve, and the amount of the refrigerant charged. The electric powers of the heaters were controlled in such a way that the refrigerants at the outlet of each pass of the evaporator were superheated at the temperature of 25°C. REFPROP was used for the thermodynamic properties of R32. Fluid flow in the header was observed by taking pictures at the recorded rate of 2,000fps with a high-speed camera through the sight glass.

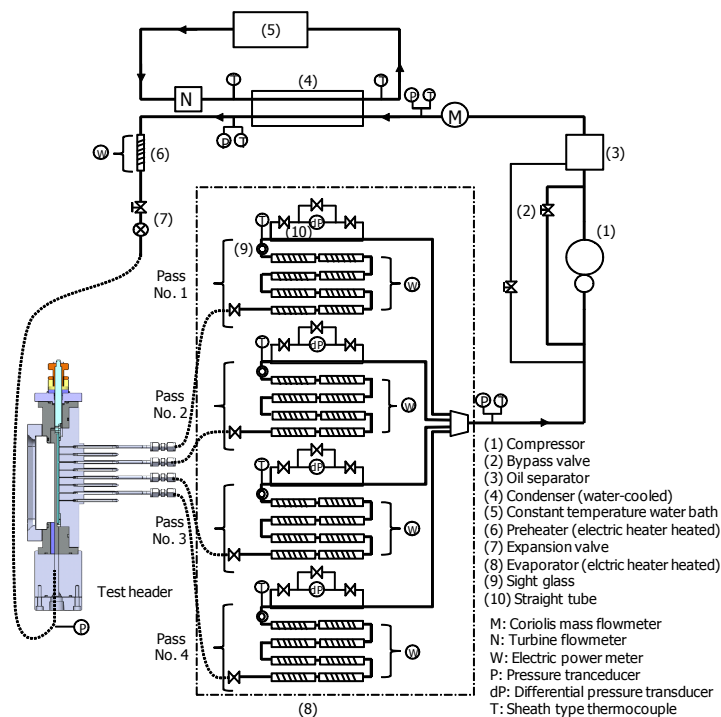


Figure 2: System diagram of experimental setup

Table 2: Test conditions at header inlet

| | |
|-----------------------|---------------------------------|
| Refrigerant | R32 |
| Pressure | 1.28MPa |
| Saturated temperature | 15°C |
| Mass flux | 25, 50, 75kg/(m ² s) |
| Quality | 0.2, 0.4, 0.6 |

3. EXPERIMENTAL RESULTS AND DISCUSSION

3.1 Effect of Inlet Quality and Mass Flux on Distribution

Figure 3 shows the measured refrigerant distribution of the header at the mass flux of 50kg/(m²s) for the standard branch pitch. The branches are numbered 1-4 from top to bottom. For the header inlet quality $x_{hi} = 0.21$, the liquid phase ratios are about 30% each for the lower three branches (No. 2-4) and only 6% for the top branch (No. 1). The liquid phase ratios for $x_{hi} = 0.37$ are about 40% each for the lower two branches (No. 3, 4), about 20% for No. 2 branch, and 2%, which is very little, for No. 1 branch. The liquid phase ratios for $x_{hi} = 0.63$ are about 60, 30, 10, and 2% for No. 4, 3, 2, and 1 branches. The liquid phase ratio of the bottom branch (No. 4) thus increases as quality increases. The liquid phase ratio of the second branch from the bottom (No. 3) once increases and then decreases and those of the top two branches (No. 1, 2) decrease monotonically as quality increases.

The branch inlet qualities for the header inlet quality $x_{hi} = 0.21$, where the liquid phase refrigerant is distributed to the lower three branches by about 30% each, are nearly zero for the lower three branches. This shows that very little vapor phase refrigerant flows into these branches. This can be found in the graph of the vapor phase ratio of branches. The branch inlet qualities for $x_{hi} = 0.37$, where the liquid phase refrigerant is distributed to the lower two branches by about 40% each, are 0.06 for the lower two branches, which is obviously very little, and this shows that liquid-rich refrigerant flows into these branches.

The vapor-liquid two-phase ratios, or the refrigerant flow rate ratios, for all qualities x_{hi} are close to 25%, which represents equal distribution. This is because the magnitude relationships of liquid phase ratio and vapor phase ratio are opposite, and as a result, the sums of liquid phase and vapor phase for each branch become nearly equal.

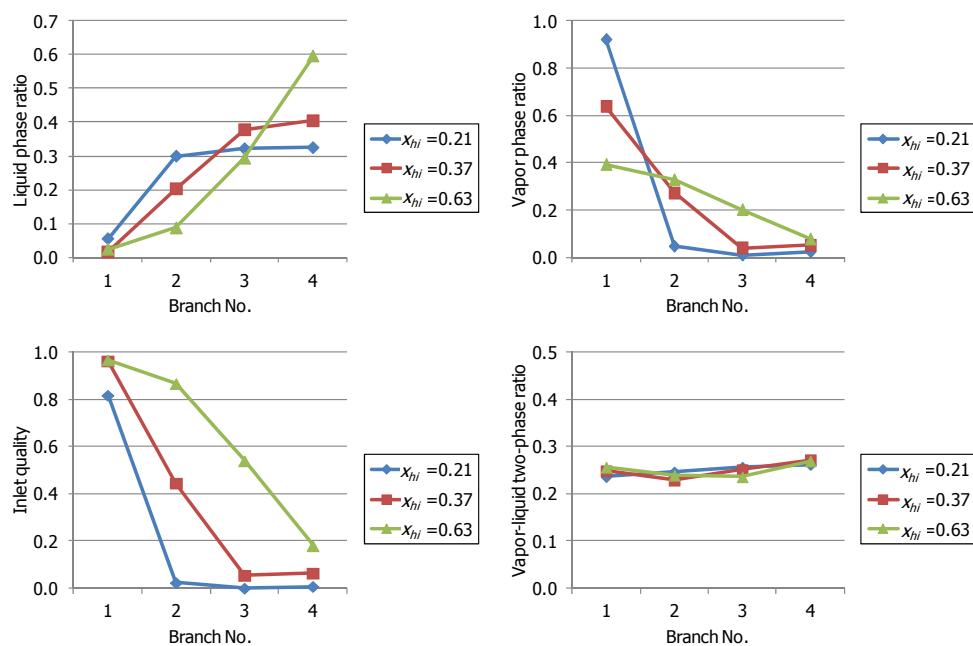
**Figure 3:** Measured refrigerant distributions of header with standard branch pitch (50kg/(m²s))

Figure 4 shows the liquid phase ratios for the mass flux of 25, 50, and 75 kg/(m²s). In the range of these mass fluxes, there is no big difference in the distribution. However, closer examination shows that as the mass flux increases, the liquid phase ratio of No. 1 branch for $x_{hi} = 0.2$ increases slightly and that of No. 4 branch for $x_{hi} = 0.6$ decreases. These show that increase in the mass flux leads in the direction of equal distribution.

Figure 5 shows the dimensional standard deviations for liquid phase distribution. For the mass flux of 50 kg/(m²s), the dimensionless standard deviation σ at $x_{hi} = 0.2$ is 45% and σ at $x_{hi} = 0.6$ is 89%, which is about twice as large as that at $x_{hi} = 0.2$. σ for the mass flux of 75 kg/(m²s) is about 10 to 20% lower than that for 50 kg/(m²s).

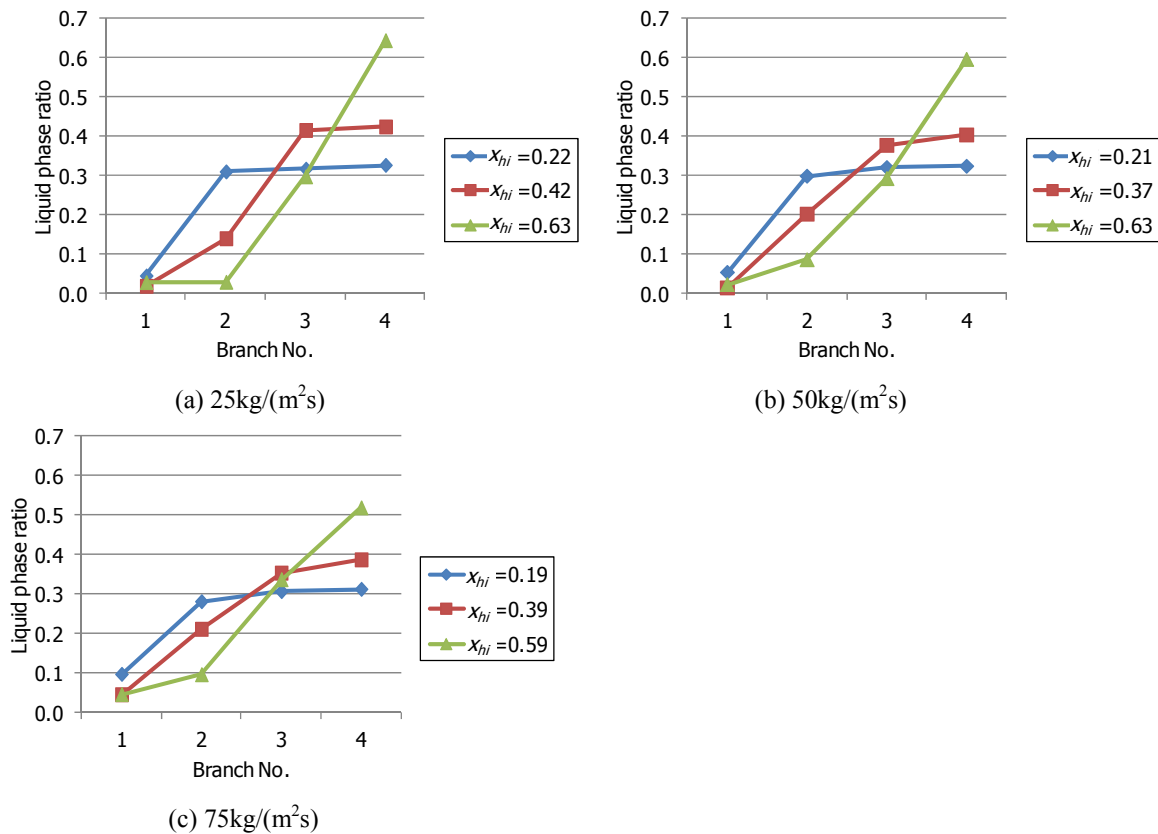


Figure 4: Effect of mass flux on liquid phase distribution

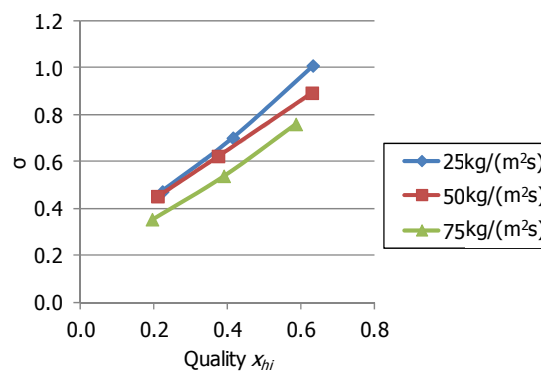


Figure 5: Relationships of inlet quality, mass flux, and dimensionless standard deviation

Figure 6 shows typical photographs of fluid flow in the header shot with the high-speed camera. The flow regime for the mass flux of 25 kg/(m²s) and the quality $x_{hi} = 0.22$ is slug flow, where liquid, which includes small bubbles, and

large bubbles flow alternately. Observation on successive photographs for one second shows that the liquid level fluctuates and rises especially largely as the large bubble rises. At this time, the liquid level exists between the top branch and the second branch from the top. The flow regime for $x_{hi} = 0.42$ is churn flow, where vapor phase flow rate increases and liquid bodies remain in places. At this time, the liquid level also fluctuates and exists between the second and third branches from the top. Since the cross-sectional shape inside the header was a rectangle and the observation was done through the one-sided glass, it is hard to determine the flow regime for $x_{hi} = 0.63$, where vapor phase flow rate is large. Under these conditions, the flow regime seems to be annular flow. At this time, the liquid level exists between the positions slightly above the second branch from the bottom and slightly above the bottom branch.

Examination of the relationship between the liquid level for the mass flux of $25\text{kg}/(\text{m}^2\text{s})$ in Figure 6 and the liquid phase distribution ratio in Figure 4(a) shows that the liquid phase refrigerant is distributed subequally to the branch almost under the liquid level. This means that for $x_{hi} = 0.22$, the liquid level is almost above the lower three branches (No. 2-4), to which the liquid phase is distributed by about 30% each, and for $x_{hi} = 0.42$, the liquid level is above the lower two branches (No.3, 4), to which the liquid phase is distributed by about 40% each.

In Figure 6, under the conditions of the mass flux larger than $50\text{kg}/(\text{m}^2\text{s})$ and the quality x_{hi} larger than 0.37, where the vapor phase speed is high, the liquid level was not able to be distinguished from the wavy liquid films formed on the glass, which had sharp fluctuation, and the height of the liquid level were not able to be determined. However, since the distributions of liquid phase ratios for the mass flux of 50 and $75\text{kg}/(\text{m}^2\text{s})$ are similar to those for $25\text{kg}/(\text{m}^2\text{s})$, the liquid levels for 50 and $75\text{kg}/(\text{m}^2\text{s})$ seem to be the same height as that for $25\text{kg}/(\text{m}^2\text{s})$.

In Figure 3, as described above, very little vapor phase refrigerant flows into the lower three branches for the quality $x_{hi} = 0.21$ and the lower two branches for $x_{hi} = 0.37$. This is because rising vapor phase does not change the flow direction, barely flowing into branch holes on the side, and goes straight upward. This is probably affected by buoyancy. Although the flow regimes depend on the mass flux and quality, little vapor phase refrigerant flows into the branch holes under the liquid level in any flow regime.

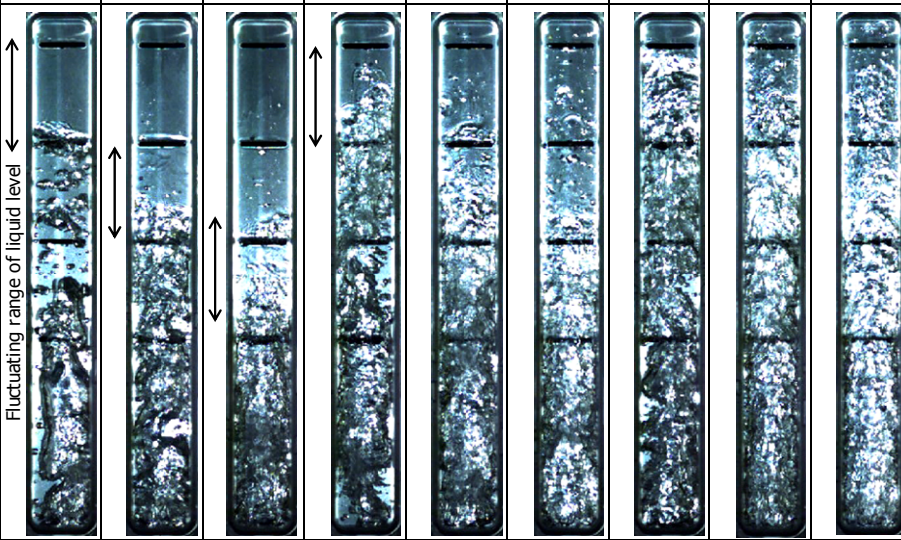
| Mass flux ($\text{kg}/(\text{m}^2\text{s})$) | 25 | | | 50 | | | 75 | | |
|---|--|------------|--------------|------------|---------------------------|--------------|---------------------------|--------------|--------------|
| Quality x_{hi} | 0.22 | 0.42 | 0.63 | 0.21 | 0.37 | 0.63 | 0.19 | 0.39 | 0.59 |
| Photograph |  | | | | | | | | |
| Flow pattern | Slug flow | Churn flow | Annular flow | Churn flow | Churn flow ~ Annular flow | Annular flow | Churn flow ~ Annular flow | Annular flow | Annular flow |

Figure 6: Photographs of flow inside header

3.2 Effect of branch pitch on distribution

Figure 7 shows the liquid phase ratios of the header with the half branch pitch for the mass flux of $25\text{kg}/(\text{m}^2\text{s})$, compared with those with the standard pitch. For the inlet quality $x_{hi} = 0.2$, although the liquid phase ratios are about 30% each for the lower three branches (No. 2-4) for the standard pitch, the ratio of No. 2 branch, which is the top, decreases slightly and the ratio of No. 1 branch increases slightly for the half pitch. For $x_{hi} = 0.4$, although the liquid phase ratios are about 40% each for the lower two branches (No. 3, 4) for the standard pitch, the ratio of No. 3 branch, which is higher, decreases slightly and the ratio of No. 2 branch increases slightly for the half pitch. Furthermore, for $x_{hi} = 0.6$, the ratio of No. 4 branch, which is the bottom, decreases and the ratio of No. 2 increases. Therefore, the decrease in branch pitch improves the distribution.

Figure 8 shows the photographs of flow inside the header with the half branch pitch. Observation on successive photographs for one second shows that the fluctuating range of liquid level of the header with the half branch pitch for each quality is almost the same or slightly larger than that with the standard branch pitch. For $x_{hi} = 0.2$, although the lowest liquid level is close to the second branch from the top (No. 2) for the header with the standard branch pitch, the lowest liquid level is close to the third branch from the top (No. 3) for the header with the half branch pitch. This leads to the increase in the ratio of the time when the liquid level is under No. 2 branch, resulting in a decrease in the liquid phase ratio of No. 2 branch. The reason for the increase in the liquid phase ratio of No. 1 branch is that the decrease in the branch pitch makes the entrained droplets reach the branch more easily. Similarly, for $x_{hi} = 0.4$, although the lowest liquid level is close to the third branch from the top (No. 3) for the header with the standard branch pitch, the lowest liquid level reaches the bottom branch (No. 4) for the header with the half branch pitch. This leads to the increase in the ratio of the time when the liquid level is under No. 3 branch, and as a result, the liquid phase ratio of No. 3 branch decreases. For $x_{hi} = 0.6$, the decrease in the branch pitch makes the entrained droplets reach No. 2 branch more easily, resulting in the increase in the liquid phase ratio of No. 2 branch.

Figure 9 shows the ratio of the dimensional standard deviations for liquid phase distribution of the header with the half branch pitch to those with the standard branch pitch. For the mass flow rate of $50\text{kg}/(\text{m}^2\text{s})$, the dimensionless standard deviations for the half branch pitch are about 20% lower in the quality range of 0.2-0.6 than those for the standard branch pitch.

The effect of branch pitch on distribution is summarized below. The fluctuating ranges of liquid level in the header are almost the same regardless of the branch pitch. As a result, the relative fluctuating range of liquid level to the branch pitch increases as the branch pitch decreases. This leads to the decrease in the liquid phase refrigerant that flows into the branch near the liquid level, and the entrained droplets reach the upper branch more easily as branch pitch decreases, resulting in improved distribution.

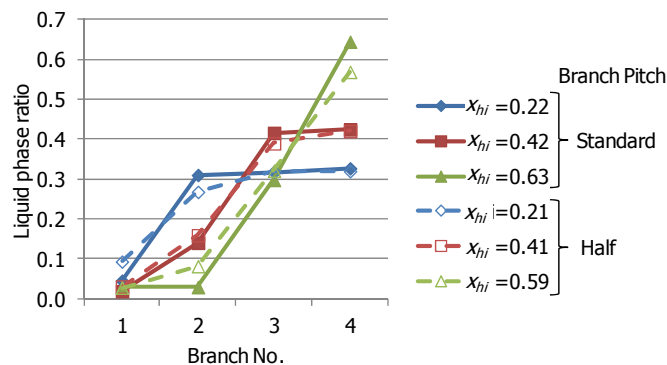


Figure 7: Effect of branch pitch on liquid phase distribution ($25\text{kg}/(\text{m}^2\text{s})$)




| Mass flux (kg/(m ² s)) | 25 | | |
|--------------------------------------|---|---|--|
| Quality x_{hi} | 0.21 | 0.41 | 0.59 |
| Photograph |  |  |  |
| Flow pattern | Slug flow | Churn flow | Annular flow |

Figure 8: Photographs of flow inside header with half branch pitch

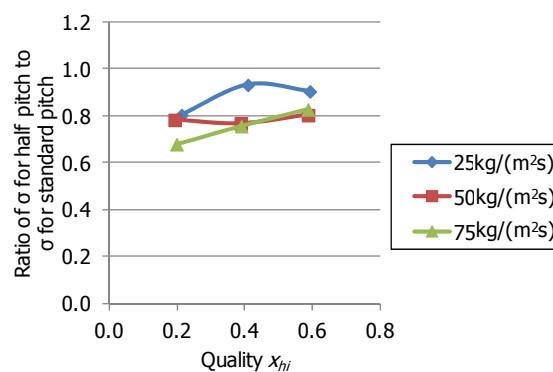


Figure 9: Effect of branch pitch on dimensionless standard deviation

6. CONCLUSIONS

The conclusions drawn from the discussion on the distribution characteristics of the vertical header on the basis of the flow visualization in the header are as follows.

- A liquid level that contains vapor phase exists in the header, and the height of the level decreases as the quality of the refrigerant increases. The amount of refrigerant that has little vapor is distributed subequally to branch holes under the level. This is because the vapor phase does not change the flow direction and rarely enters the branch holes on the side due to the effect of buoyancy.
- The fluctuating ranges of liquid level in the header are almost the same regardless of the branch pitch. As a result, the relative fluctuating range of liquid level to the branch pitch increases as the branch pitch decreases. This leads to

the decrease in the liquid phase refrigerant that flows into the branch near the liquid level, and the entrained droplets reach the upper branch more easily as branch pitch decreases, resulting in improved distribution.

NOMENCLATURE

| | | | |
|------------|----------------------------------|----------------------|--------------------------|
| C_p | Heat capacity | (J/(kgK)) | Subscript |
| i | Enthalpy | (J/kg) | c Condenser |
| G | Mass flow rate | (kg/s) | e Evaporator |
| k | Correction factor | (-) | h Header |
| L | Volume flow rate | (m ³ /s) | i Inlet, branch number |
| Q | Heat exchange amount | (W) | l Liquid |
| T | Temperature | (°C) | o Outlet |
| W | Electric power of heater | (W) | ph Preheater |
| x | Quality | (-) | r Refrigerant |
| ΔP | Differential pressure | (Pa) | v Vapor |
| μ | Viscosity | (Pa-s) | w Water |
| ρ | Density | (kg/m ³) | |
| σ | Dimensionless standard deviation | (-) | |

REFERENCES

- Byun, H. W., Kim, N. H. (2011). Refrigerant distribution in a parallel flow heat exchanger having vertical headers and heated horizontal tubes. *Exp. Therm. Fluid Sci.*, 35, 920-932.
- Lee, J. K. (2009). Two-phase flow behavior inside a header connected to multiple parallel channels. *Exp. Therm. Fluid Sci.*, 33, 195-202.
- Lemmon, E. W., Huber, M. L., McLinden, M. O. (2013). *NIST Standard Reference Database 23: Reference Fluid Thermodynamic and Transport Properties-REFPROP*, Version 9.1, National Institute of Standards and Technology, Standard Reference Data Program, Gaithersburg.
- Zou, Y., Hrnjak, P. S. (2013). Refrigeration distribution in the vertical header of the microchannel heat exchanger – Measurement and visualization of R410A flow. *Int. J. Refrig.*, 36, 2196-2208.
- Zou, Y., Hrnjak, P. S. (2015). Distribution function for reversible microchannel heat exchanger with vertical headers – Considering the effects of inlet conditions, geometries and fluid properties. *Proceedings of the 24th International Congress of Refrigeration, Yokohama, Japan* (ID: 6). Paris, France: IIR.